

Transversity GPD in photoproduction and electroproduction of two vector mesons

R. Enberg^{1,2,a}, B. Pire¹, L. Szymanowski^{3,4,5}

¹ CPhT, École Polytechnique, 91128 Palaiseau, France^b

² Lawrence Berkeley National Laboratory, Berkeley, CA 94720, USA

³ Soltan Institute for Nuclear Studies, Hoża 69, 00-681 Warsaw, Poland

⁴ Université de Liège, 4000 Liège, Belgium

⁵ LPT, Université Paris-Sud, 91405 Orsay, France^c

Received: 18 January 2006 / Revised version: 11 March 2006 /
 Published online: 20 April 2006 – © Springer-Verlag / Società Italiana di Fisica 2006

Abstract. The chiral-odd generalized parton distribution (GPD), or transversity GPD, of the nucleon can be accessed experimentally through the photoproduction or electroproduction of two vector mesons on a polarized nucleon target, $\gamma^{(*)}N \rightarrow \rho_1\rho_2N'$, where ρ_1 is produced at large transverse momentum, ρ_2 is transversely polarized, and the mesons are separated by a large rapidity gap. We predict the cross section for this process for both transverse and longitudinal ρ_2 production. To this end, we propose a model for the transversity GPD $H_T(x, \xi, t)$ and give an estimate of the relative sizes of the transverse and longitudinal ρ_2 cross sections. We show that a dedicated experiment at high energy should be able to measure the transversity content of the proton.

1 Introduction

Accessing the chiral-odd quark content of the proton has a long history [1], which has been detailed elsewhere [2]. The particular case of the chiral-odd generalized parton distributions is interesting in itself [3]. Following the previous work in [4], we consider here the process¹

$$\gamma_{L/T}^{(*)}p \rightarrow \rho_L^0\rho_{L/T}^+n \quad (1)$$

shown in Fig. 1, that is, virtual or real photoproduction on a proton p , which leads via two-gluon exchange to the production of a longitudinally polarized vector meson ρ_L^0 separated by a large rapidity gap from another longitudinally or transversely polarized vector meson $\rho_{L/T}^+$ and the scattered neutron n . We consider the kinematical region where the rapidity gap between ρ^+ and n is much smaller than the one between ρ^0 and ρ^+ , that is the energy of the system ($\rho^+ - n$) is smaller than the energy of the system ($\rho^0 - \rho^+$) but, to justify our approach, is still larger than baryonic resonance masses.

^a e-mail: REnberg@lbl.gov

^b Unité mixte 7644 du CNRS

^c Unité mixte 8627 du CNRS

¹ The process $\gamma^*p \rightarrow \rho_1^0\rho_2^0p$ may equally well be discussed along the same lines, since its amplitude is described by exactly the same graphs, due to charge conjugation invariance, which forbids contribution of the gluonic GPDs.

We have previously shown [4] that in such kinematical circumstances the Born term for this process can be consistently calculated using the collinear QCD factorization method. The final result is represented as an integral (over the longitudinal momentum fractions of the quarks) of the product of two amplitudes. The first one describes the transition $\gamma^{(*)} \rightarrow \rho_L^0$ via two-gluon exchange, which can be also viewed as the Born approximation of a hard pomeron. The second one describes the two gluon (pomeron)–proton subprocess $\mathbb{P}p \rightarrow \rho^+n$, which is closely related to the electroproduction process $\gamma^*N \rightarrow \rho N'$, where collinear factorization theorems allow separating the long distance dynamics expressed through the GPDs from a perturbatively calculable coefficient function. The hard scale appearing in the process in Fig. 1 is supplied by the relatively large momentum transfer in the two-gluon channel, i.e. by the virtuality of the “pomeron”.

The first process that we will calculate is the one with both vector mesons longitudinally polarized,

$$\gamma^{(*)}(q)p(p_2) \rightarrow \rho_L^0(q_\rho)\rho_L^+(p_\rho)n(p'_2), \quad (2)$$

which involves the emission of two gluons in the $\gamma \rightarrow \rho_L$ transition. We choose a charged vector meson ρ^+ to select quark–antiquark exchange with the nucleon line. The second process that we are interested in is the one involving the chiral-odd GPD, e.g.

$$\gamma^{(*)}(q)p(p_2) \rightarrow \rho_L^0(q_\rho)\rho_T^+(p_\rho)n(p'_2), \quad (3)$$

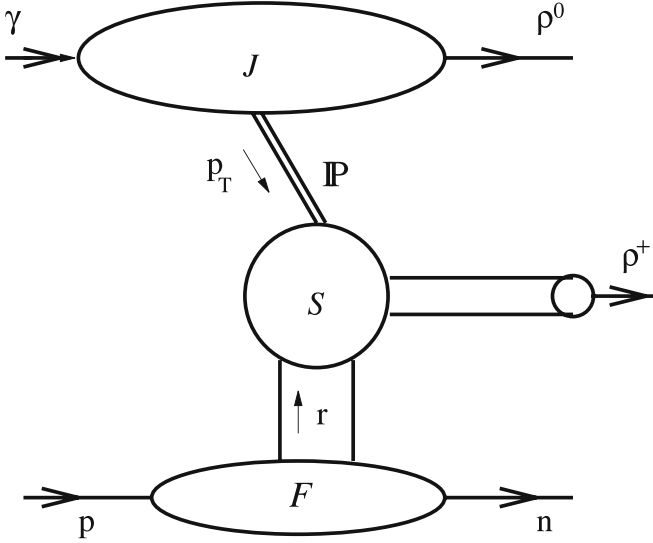


Fig. 1. Factorization of the process $\gamma_{L/T}^{(*)} p \rightarrow \rho_L^0 \rho_{L/T}^+ n$ in the asymmetric kinematics discussed in the text. \mathbb{P} describes the two-gluon exchange (Born approximation of the hard pomeron)

which is the main motivation for the study of this two-meson production process.

2 Kinematics

Let us first summarize the details of the kinematics of the process, restricting ourselves to real photoproduction. We introduce two light-like Sudakov vectors p_1 and $P = 1/2(p_2 + p_{2'})$. We also introduce the auxiliary variable $\mathcal{S} = 2p_1 P$, related to the total center-of-mass energy squared of the $\gamma^* p$ -system, $s = (q + p_2)^2$, as $s + Q^2 = (1 + \xi)\mathcal{S}$. The momenta are parameterized as follows:

$$\begin{aligned} q^\mu &= p_1^\mu - \frac{Q^2}{\mathcal{S}} P^\mu, & q_\rho^\mu &= \alpha p_1^\mu + \frac{\mathbf{p}^2}{\alpha \mathcal{S}} P^\mu + p_T^\mu, \\ p_T^2 &= -\mathbf{p}^2, & p_\rho^\mu &= \bar{\alpha} p_1^\mu + \frac{\mathbf{p}^2}{\bar{\alpha} \mathcal{S}} P^\mu - p_T^\mu, \\ \bar{\alpha} &\equiv 1 - \alpha, & p_2^\mu &= (1 + \xi) P^\mu, & p_{2'}^\mu &= (1 - \xi) P^\mu, \end{aligned} \quad (4)$$

where $Q^2 = -q^2$ is the photon virtuality, and ξ is the skewedness parameter, which can be written in terms of the invariant mass s_1 of the two mesons as

$$\xi = \frac{s_1 + Q^2}{2\mathcal{S}}, \quad s_1 = (q_\rho + p_\rho)^2 = \frac{\mathbf{p}^2}{\alpha \bar{\alpha}}. \quad (5)$$

The ρ^+ -meson–target invariant mass equals

$$s_2 = (p_\rho + p_{2'})^2 = \mathcal{S} \bar{\alpha} (1 - \xi). \quad (6)$$

The kinematical limit with a large rapidity gap between the two mesons in the final state is obtained by demanding that s_1 be very large, of the order of $\mathcal{S} \approx s$,

$$s_1 = 2\mathcal{S} \xi, \quad s_1 \gg \mathbf{p}^2, \quad (7)$$

whereas s_2 is kept to the order of \mathbf{p}^2 ,

$$s_2 \rightarrow \frac{\mathbf{p}^2}{2\xi} (1 - \xi), \quad (8)$$

large enough to justify the use of perturbation theory in the collinear subprocess $\mathbb{P} p \rightarrow \rho^+ n$ and the application of the GPD framework.

In terms of the longitudinal fraction α , the limit with a large rapidity gap corresponds to taking the limits

$$\alpha \rightarrow 1, \quad \bar{\alpha} s_1 \rightarrow \mathbf{p}^2, \quad \xi \sim 1. \quad (9)$$

We choose the kinematics so that the nucleon gets no transverse momentum in the process. The t -dependence of the GPDs is not known in detail, but the sum rules that relate it to the nucleon form factors imply a strong decrease of the cross section with increasing $-t$. Thus, taking $t = t_{\min}$ yields simpler formulas and amounts to most of the cross section. One may, however, allow a finite momentum transfer, small with respect to $|\mathbf{p}|$, correcting expressions of the amplitude with contributions containing additional GPDs.

Let us repeat that the role of the main hard scale in the processes under discussion below is played by the virtuality $p^2 = -\mathbf{p}^2$, which is the large momentum transfer in the two-gluon exchange channel.

The three-particle phase space needed to obtain the differential cross section is computed through the standard recurrence relation, which gives

$$d\text{PS}_3(s, p_2, p_\rho, p_{2'}) = \frac{1}{256\pi^4 s s_2} dp_T^2 dt ds_2 d\Phi, \quad (10)$$

where Φ is the angle between the $(\gamma\rho^0)$ plane and the (p, n, ρ^+) plane. At $t = t_{\min}$, this angle is irrelevant and the phase space factor simplifies to

$$d\text{PS}_3(s, p_2, p_\rho, p_{2'}) = \frac{1}{128\pi^3 s \xi (1 - \xi)} dp_T^2 dt d\xi. \quad (11)$$

The differential cross section at the minimal value of $-t = -t_{\min}$ then reads

$$\frac{d\sigma}{dp_T^2 dt d\xi} = \frac{1}{256\pi^3 \xi (1 - \xi) s^2} |\mathcal{M}|^2. \quad (12)$$

3 The scattering amplitude

The scattering amplitude \mathcal{M} of the process (2) using the standard collinear QCD factorization method is written in a form suggested by Fig. 1 as:

$$\begin{aligned} \mathcal{M} &\sim \sum_{q=u,d} \int_0^1 dz \int_0^1 du \int_{-1}^1 dx \\ &\quad \times T_H^q(x_1, u, z) H^q(x, \xi, 0) \phi_{\rho^+}(u) \phi_{\rho^0}(z). \end{aligned} \quad (13)$$

Here $H^q(x, \xi, 0)$ is the generalized parton distribution of parton q in the target at zero momentum transfer and $x + \xi$ and $\xi - x$ are (see Fig. 1) the momentum fractions of the quark and antiquark emitted by the target (since it turns out that our kinematics selects $x < \xi$, the second parton is interpreted as an emitted antiquark). $\phi_{\rho^+}(u)$ and $\phi_{\rho^0}(z)$ are the distribution amplitudes (DA) of the ρ^+ -meson and ρ^0 -meson, respectively, and u and z are the corresponding lightcone momentum fractions of the quark in the meson. We will also use the shorthand notation $\bar{z} = 1 - z$ and $\bar{u} = 1 - u$ in the following. $T_H^q(x, u, z)$ is the hard scattering amplitude (the coefficient function). For clarity of notation in (13) we omit the factorization scale dependence of T_H^q , H^q , ϕ_{ρ^0} and ϕ_{ρ^+} .

Equation 13 describes the amplitude in the leading twist approximation. In other words, all terms suppressed by powers of a hard scale parameter $1/|\mathbf{p}|$ are omitted. Within this approximation one neglects (in the physical gauge) the contributions of higher Fock states in the meson wave functions and many parton correlations (higher twist GPDs) in the proton. Moreover, we also use the collinear approximation: in the hard scattering amplitude we neglect the relative transverse momenta (with respect to the meson momentum) of the constituent quarks. These approximations result in the appearance of the distribution amplitudes in the factorization formula (13), i.e. the lightcone wave functions, integrated over the relative transverse momenta of constituents up to the collinear factorization scale.

An additional simplification appears in the kinematics given by (7–9). In this limit one needs consider only the diagrams that involve two-gluon exchange between the two mesons. The other contributions (the fermion exchange diagrams) to the coefficient function T_H^p are known [5] to be suppressed by powers of \mathbf{p}^2/s . Therefore, we will not discuss them here. With the same accuracy, i.e. neglecting terms $\sim \mathbf{p}^2/s$, the contribution of gluon exchange diagrams shown in Fig. 2 turns out to be purely imaginary. It involves GPDs in the ERBL region $-\xi < x < \xi$ only, which is quite specific for our process [4].

The amplitude may then be written in terms of the impact factor $J^{\gamma_{L/T}^* \rightarrow \rho_L^0}$ as

$$\begin{aligned} \mathcal{M}^{\gamma_{L/T}^* p \rightarrow \rho_L^0 \rho_L^+ n} &= i16\pi^2 s \alpha_s f_\rho^+ \xi \sqrt{\frac{1-\xi}{1+\xi}} \frac{C_F}{N(\mathbf{p}^2)^2} \\ &\times \int_0^1 \frac{du \phi_{\parallel}(u)}{u^2 \bar{u}^2} J^{\gamma_{L/T}^* \rightarrow \rho_L^0}(u\mathbf{p}, \bar{u}\mathbf{p}) \\ &\times \left[H^u(\xi(2u-1), \xi, 0) \right. \\ &\quad \left. - H^d(\xi(2u-1), \xi, 0) \right]. \end{aligned} \quad (14)$$

The impact factor $J^{\gamma_{L/T}^* \rightarrow \rho_L^0}$ has the form

$$J^{\gamma_{L/T}^* \rightarrow \rho_L^0}(\mathbf{k}_1, \mathbf{k}_2) = -f_\rho \frac{e\alpha_s 2\pi Q}{N_c \sqrt{2}} \int_0^1 dz z \bar{z} \phi_{\parallel}(z) P(\mathbf{k}_1, \mathbf{k}_2), \quad (15)$$

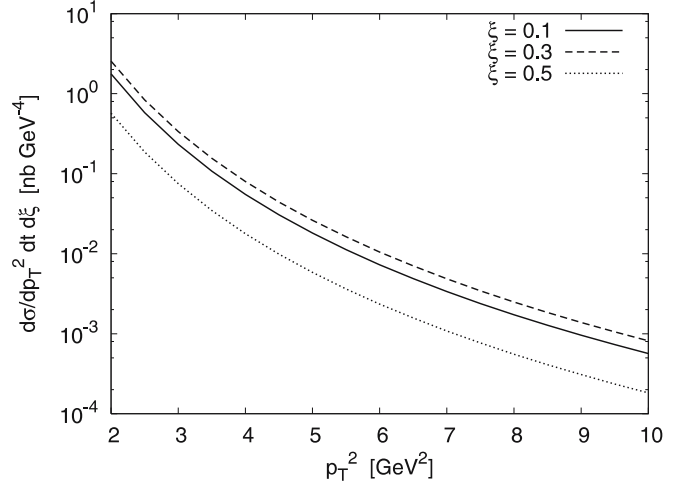


Fig. 2. The differential cross section for the photoproduction of longitudinally polarized ρ^0 and ρ^+ as a function of the squared transverse momentum p_T^2 for $\xi = 0.1, 0.3$, and 0.5

with the $\phi_{\parallel}(z)$ DA defined by the matrix element

$$\begin{aligned} \langle 0 | \bar{q}(0) \gamma^\mu q(y) | \rho_L^0(q_\rho) \rangle &= q_\rho^\mu f_\rho^0 \int_0^1 dz \\ &\times e^{-iz(q_\rho y)} \phi_{\parallel}(z). \end{aligned} \quad (16)$$

For $\gamma^{(*)}$ transversely polarized, $J^{\gamma_{T}^* \rightarrow \rho_L^0}$ reads:

$$\begin{aligned} J^{\gamma_{T}^* \rightarrow \rho_L^0}(\mathbf{k}_1, \mathbf{k}_2 = \mathbf{p} - \mathbf{k}_1) &= -\frac{e\alpha_s \pi f_\rho^0}{\sqrt{2} N} \int_0^1 dz \\ &\times (2z-1) \phi_{\parallel}(z) (\varepsilon \mathbf{Q}_P). \end{aligned} \quad (17)$$

Here ε is the polarization vector of the initial photon,

$$\begin{aligned} P(\mathbf{k}_1, \mathbf{k}_2 = \mathbf{p} - \mathbf{k}_1) &= \\ &\frac{1}{z^2 \mathbf{p}^2 + m_q^2 + Q^2 z \bar{z}} + \frac{1}{\bar{z}^2 \mathbf{p}^2 + m_q^2 + Q^2 z \bar{z}} \\ &- \frac{1}{(\mathbf{k}_1 - z\mathbf{p})^2 + m_q^2 + Q^2 z \bar{z}} - \frac{1}{(\mathbf{k}_1 - \bar{z}\mathbf{p})^2 + m_q^2 + Q^2 z \bar{z}}, \end{aligned} \quad (18)$$

and

$$\begin{aligned} \mathbf{Q}_P(\mathbf{k}_1, \mathbf{k}_2 = \mathbf{p} - \mathbf{k}_1) &= \\ &\frac{z\mathbf{p}}{z^2 \mathbf{p}^2 + Q^2 z \bar{z} + m_q^2} - \frac{\bar{z}\mathbf{p}}{\bar{z}^2 \mathbf{p}^2 + Q^2 z \bar{z} + m_q^2} \\ &+ \frac{\mathbf{k}_1 - z\mathbf{p}}{(\mathbf{k}_1 - z\mathbf{p})^2 + Q^2 z \bar{z} + m_q^2} - \frac{\mathbf{k}_1 - \bar{z}\mathbf{p}}{(\mathbf{k}_1 - \bar{z}\mathbf{p})^2 + Q^2 z \bar{z} + m_q^2}. \end{aligned} \quad (19)$$

In all our estimates in this paper we put the quark mass $m_q = 0$.

In the case of the transversely polarized ρ_T^+ meson production, one instead gets

$$\begin{aligned} \mathcal{M}^{\gamma_{L/T}^{(*)} p \rightarrow \rho_L^0 \rho_T^+ n} &= -\sin\theta \, 16\pi^2 s \alpha_s f_\rho^T \xi \sqrt{\frac{1-\xi}{1+\xi}} \frac{C_F}{N(\mathbf{p}^2)^2} \\ &\times \int_0^1 \frac{du \, \phi_\perp(u)}{u^2 \bar{u}^2} J^{\gamma_{L/T}^{(*)} \rightarrow \rho_L^0}(u\mathbf{p}, \bar{u}\mathbf{p}) \\ &\times \left[H_T^u(\xi(2u-1), \xi, 0) \right. \\ &\quad \left. - H_T^d(\xi(2u-1), \xi, 0) \right], \quad (20) \end{aligned}$$

which involves the chiral-odd transversity distribution whose investigation is the main motivation of our studies. $J^{\gamma_{L/T}^{(*)} \rightarrow \rho_L^0}$ are the same impact factors as in (14), and θ is the angle between the transverse polarization vector of the target \mathbf{n} and the polarization vector ϵ_T of the produced ρ_T^+ -meson. In our numerical studies, we use $\theta = \pi/2$, but this dependence should of course be confirmed experimentally.

The chiral-odd light-cone distribution amplitude for the transversely polarized ρ -meson is defined by the matrix element [6]

$$\begin{aligned} \langle \rho_T(p_\rho, T) | \bar{q}(x) \sigma^{\mu\nu} q(-x) | 0 \rangle &= i f_\rho^T (p_\rho^\mu \epsilon_T^{*\nu} - p_\rho^\nu \epsilon_T^{*\mu}) \\ &\times \int_0^1 du \, e^{-i(2u-1)(p_\rho x)} \phi_\perp(u). \quad (21) \end{aligned}$$

We use the asymptotic forms of both ρ_T^+ and ρ_L^0 DAs, i.e. $\phi_\perp(u) = \phi_\parallel(u) = 6u\bar{u}$.

We use the values of the meson decay constants in the above expressions at the scale 1 GeV: $f_\rho^+ = 198 \pm 7$ MeV for the longitudinal ρ^+ , $f_\rho^0 = 216 \pm 5$ MeV for the longitudinal ρ^0 , and $f_\rho^T = 160 \pm 10$ MeV for the transverse ρ^+ .

The generalized transversity distribution in the nucleon target described by the polarization vector n^μ is defined by the formula [7]

$$\begin{aligned} \int \frac{dz^-}{4\pi} e^{ixP^+ z^-} \langle N(p_2', n) | \bar{q}(-\frac{z}{2}) i\sigma^+ i q(\frac{z}{2}) | N(p_2, n) \rangle &= \\ \frac{1}{2P^+} \bar{u}(p_2', n) i\sigma^+ i u(p_2, n) H_T^q(x, \xi, t), \quad (22) \end{aligned}$$

where terms vanishing at $t = t_{\min}$ (i.e. $\Delta_T = 0$) have been neglected. Our convention is $\sigma^{\mu\nu} = i/2[\gamma^\mu, \gamma^\nu]$.

Finally, two remarks are in order. Note that as $|\mathcal{M}|^2$, both from (14) and (20), is proportional to s^2 , the s -dependence cancels in the full cross section (12). We want to stress that this is valid only for the high energy limit discussed in Sect. 2. If one is willing to study these processes at lower energy, one should include all polarization states of exchanged gluons² and the additional contributions related to quark exchanges.

² At high energies the longitudinal polarization states of t -channel gluons (or in the Regge theory language the ‘‘nonsense’’ polarizations) give the dominant contribution and we omit the contribution of other polarization states.

4 The longitudinally polarized meson case

Let us first estimate the rate in the longitudinally polarized meson case. As in other ρ -meson production processes, the dominant contribution comes from the unpolarized GPD $H(x, \xi, t)$ and we will neglect the $E(x, \xi, t)$ contributions that vanish at $t = t_{\min}$. Our process selects the isovector part of this GPD. We use a standard description of this GPD in terms of double distributions, due to Radyushkin [8]. In general, it should be supplemented by a D-term [9] contribution. Since the chiral quark model estimates show that this latter term is almost flavor independent [10], we will not include it in our model calculation involving isovector GPDs. We thus assume

$$\begin{aligned} H(x, \xi, t) &= \\ &\frac{\theta(\xi+x)}{1+\xi} \int_0^{\min[\frac{\xi+x}{2\xi}, \frac{1-x}{1-\xi}]} dy F^q\left(\frac{\xi+x-2\xi y}{1+\xi}, y, t\right) \\ &- \frac{\theta(\xi-x)}{1+\xi} \int_0^{\min[\frac{\xi-x}{2\xi}, \frac{1+x}{1-\xi}]} dy F^q\left(\frac{\xi-x-2\xi y}{1+\xi}, y, t\right), \quad (23) \end{aligned}$$

where the double distribution $F^q(X, Y, t)$ is given by the ansatz [8]

$$F^q(X, Y, t) = \frac{F_1^q(t)}{F_1^q(0)} q(X) 6 \frac{Y(1-X-Y)}{(1-X)^3}. \quad (24)$$

In the expression (24), $q(X)$ is the quark parton distribution function, for which we use the parameterization of [11]. The t -dependence of the GPDs is given by the functions $F_1^q(t)$, which are related to the electromagnetic form factors of the proton and neutron, but since we are only evaluating the amplitudes at $t = t_{\min}$ their form is not important.

To compute the cross sections we must, in general, evaluate the integrals over u and z numerically; in the photo-

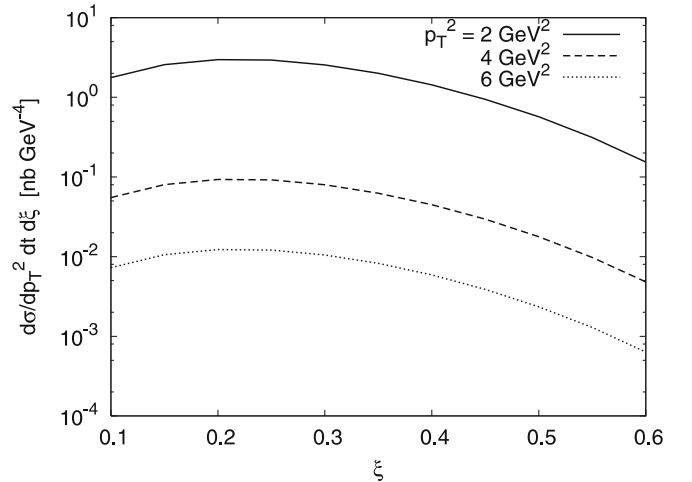


Fig. 3. The differential cross section for the photoproduction of longitudinally polarized ρ^0 and ρ^+ as a function of ξ for $p_T^2 = 2, 4, \text{ and } 6 \text{ GeV}^2$

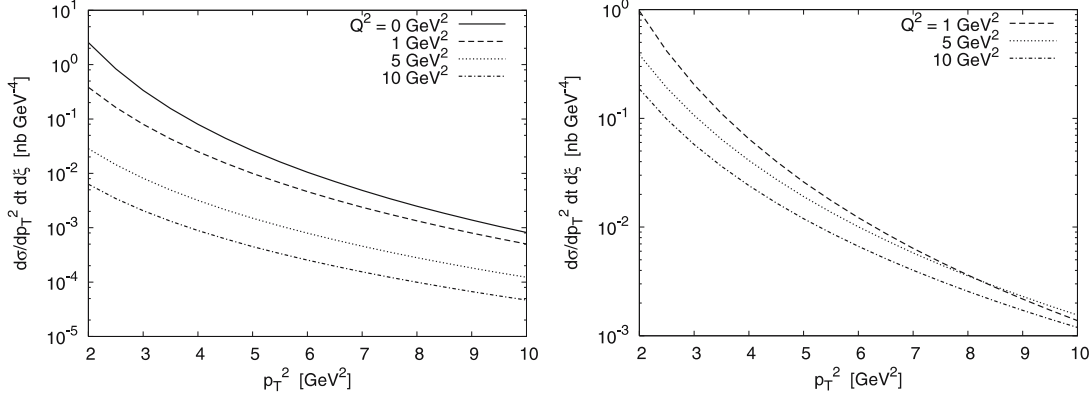


Fig. 4. The differential cross section for $\gamma_{L/T}^*(Q)p \rightarrow \rho_L^0 \rho_T^+ n$ for the transverse virtual photon (*left*) and the longitudinal virtual photon (*right*), plotted as a function of p_T^2 for $\xi = 0.3$ and $Q^2 = 0, 1, 5,$ and 10 GeV^2

production case, care must be taken to properly treat the apparent divergences at $u = z$ and $u + z = 1$.

The differential cross section for longitudinally polarized ρ^+ production is shown in Figs. 2, 3 and 4 for the real and virtual photon cases. We conclude from these figures that the photoproduction rate is much larger than the electroproduction rate (note that we did not include the additional suppression factor coming from the virtual photon flux and instead show the transverse and longitudinal photon cases separately).

5 Modeling the transversity GPD

To estimate the rate of our process in the case of transversely polarized ρ^+ , we need to formulate a model for the transversity dependent GPD $H_T(x, \xi, t)$. From (20) it follows that we only need a model for the transversity GPD in the ERBL region, $-\xi \leq x \leq \xi$. Unfortunately, even in the case of the forward h_1 structure function only very rough bag model estimates are available [12]. The bag model estimate of the leading transversity GPD was given recently in [13]. Recent progress was also made with lattice methods that have estimated its first x moments [14].

We propose a simple model inspired by [15], in which the \tilde{E} GPD was evaluated within the chiral approach, where a meson exchange dominates the physical process encoded in the GPD. The analogous meson pole approach was applied in the case of the forward transversity distribution in [16]. Below we generalize the pole model of the nucleon tensor charge developed in [16] to non-forward kinematics.

We start with the effective interaction Lagrangian

$$\mathcal{L}_{ANN} = \frac{g_{ANN}}{2M} \bar{N} \sigma_{\mu\nu} \gamma_5 \partial^\nu A^\mu N, \quad (25)$$

in which g_{ANN} is the coupling constant determining the strength of the interaction of the axial meson A with the nucleon N . Inserting the interaction term $i \int d^4x \mathcal{L}_{ANN}$ into the S -matrix element in the left-hand side of (22) and using the reduction formula, one can separate the contribution to H_T of the axial meson pole. In this way, for transversely polarized nucleons described by the polarization vector $S_T = (0, \mathbf{n}_\perp, 0)$, using the definition (22) of H_T^q ,

we get the non-forward version of (7) of [16] as

$$H_T^a(x, \xi) = \frac{g_{ANN} f_A^{a\perp} (\Delta \cdot S_T)^2}{2M_N m_A^2} \frac{\phi_\perp(\frac{x+\xi}{2\xi})}{2\xi}, \quad (26)$$

where Δ is the transverse part of the momentum transfer vector r (see Fig. 1) and $f_A^{a\perp}$ is related to the A -meson decay constant. We have here used the definition [6] of the transversely polarized axial vector meson distribution amplitude,

$$\begin{aligned} & \langle 0 | \bar{q}(-1/2z) \sigma^{\alpha\beta} \gamma_5 \frac{\lambda^a}{2} q(1/2z) | A(k, \lambda) \rangle = \\ & i f_A^{aT} [\epsilon^\alpha(\lambda) k^\beta - \epsilon^\beta(\lambda) k^\alpha] \int_0^1 du e^{i/2(1-2u)k \cdot z} \phi_\perp^A(u), \end{aligned} \quad (27)$$

in which $\epsilon(\lambda)$ is the polarization vector of meson A with the momentum k , and $\phi_\perp^A(z)$ is the distribution amplitude. To obtain (26) it is useful to note that the definition (22) can be rewritten using the Dirac structure $\sigma^{+j} \gamma_5$ instead of $i\sigma^{+i}$ [7].

According to the model of [16], we now identify the scalar product $(\Delta \cdot S_T)^2$ with the average of the intrinsic transverse momentum of the quarks: $(\Delta \cdot S_T)^2 \rightarrow 1/2 \langle k_\perp^2 \rangle$. Also, the valence quantum number of t -channel isovector exchange leads to the identification of the axial meson as $A = b_1(1235)$. In this way, using the $SU(2)$ relation

$$\langle n | \bar{d} O u | p \rangle = \langle p | \bar{u} O u | p \rangle - \langle p | \bar{d} O d | p \rangle, \quad (28)$$

we obtain as the final expression for the valence part $H_T^v = H_T^u - H_T^d$ (compare with (12) of [16])

$$H_T^v(x, \xi, t) = \frac{g_{b_1 NN} f_{b_1}^T \langle k_\perp^2 \rangle}{2\sqrt{2} M_N m_{b_1}^2} \frac{\phi_\perp^{b_1}(\frac{x+\xi}{2\xi})}{2\xi}, \quad (29)$$

where, according to (8), (9), and (10) of [16],

$$\begin{aligned} f_{b_1}^T &= \frac{\sqrt{2}}{m_{b_1}} f_{a_1}, & f_{a_1} &= (0.19 \pm 0.03) \text{ GeV}^2, \\ g_{b_1 NN} &= \frac{5}{3\sqrt{2}} g_{a_1 NN}, & g_{a_1 NN} &= 7.49 \pm 1.0, \end{aligned} \quad (30)$$

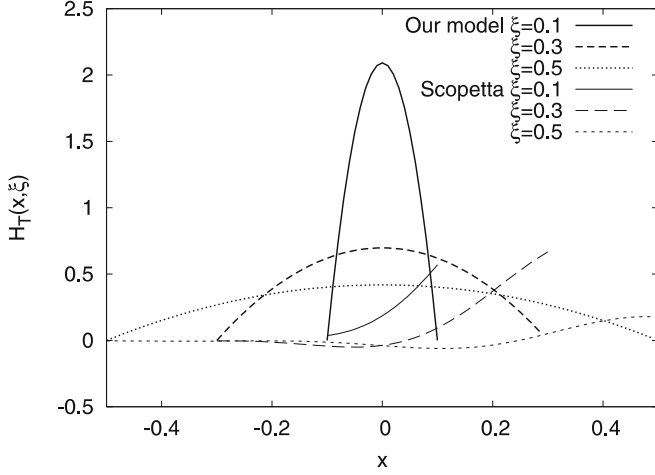


Fig. 5. The transversity GPD $H_T(x, \xi, 0)$ for various values of ξ for x in the ERBL region, in our model (*thicker curves*) and in the model of [13] (*thinner curves*)

and

$$\langle k_\perp^2 \rangle = (0.58 \div 1.0) \text{ GeV}^2. \quad (31)$$

(We use the lower value $\langle k_\perp^2 \rangle = 0.58$ in our numerical estimates). In the following, we assume that the distribution amplitude $\phi_\perp^{b_1}$ takes its asymptotic form, $\phi_\perp^{b_1}(u) = 6u\bar{u}$. In Fig. 5 we show the resulting transversity GPD $H_T(x, \xi, 0)$ for various values of ξ .

The second model used in our estimates is the bag model estimate of [13]. In Fig. 5 we also show the comparison of this transversity GPD with the one defined by (29). We see that these models lead to quite different results, which can consequently serve as an estimate of theoretical uncertainties of our rate estimates. We want to stress that quark models, such as in [13], naturally underestimate the GPDs in the ERBL region, since they do not include the physics of meson exchange, which is at the core of our model.

6 Cross sections for $\rho_L^0 \rho_T^+$ production

Let us now estimate the rates for the production of the transversely polarized ρ_T^+ -meson and discuss the feasibility of measuring the transversity GPD in the proposed process. We first note that since the analytic expression (29) for the chiral-odd GPD is rather simple, we can compute, in the case of photoproduction, the integral over u in (20) analytically. One obtains³

$$\mathcal{M}^{\gamma p \rightarrow \rho_L^0 \rho_T^+ n} |_{Q^2=0} = \sin\theta \frac{216 \pi^3 s \alpha_s^2 e C_F}{N_c^2} \times \frac{g_{b_1 NN} f_\rho^T f_\rho^0 f_{b_1}^T \langle k_\perp^2 \rangle}{M_p m_{b_1}^2} \sqrt{\frac{1-\xi}{1+\xi}} \frac{1}{|\mathbf{p}|^5}, \quad (32)$$

³ We emphasize that this result holds for our simple model estimate of the chiral-odd GPD, and not for a more complete treatment.

and, therefore, for the cross section

$$\frac{d\sigma}{dp_T^2 dt d\xi} = \frac{729 \pi^4 \alpha_s^4 \alpha_{em} C_F^2}{N_c^4} \frac{\left[g_{b_1 NN} f_\rho^T f_\rho^0 f_{b_1}^T \langle k_\perp^2 \rangle \right]^2}{M_p^2 m_{b_1}^4} \times \frac{\sin^2 \theta}{\xi(1+\xi)|\mathbf{p}|^{10}}. \quad (33)$$

For $Q^2 > 0$ we evaluate the integrals numerically. The cross section for the transversely polarized ρ case has a characteristic $\sin^2 \theta$ -dependence (see (20)), which we do not explore here.

The differential cross sections for real and virtual photoproduction of transversely polarized ρ^+ , based on (33), are shown in Figs. 6, 7 and 8. As for the longitudinal ρ_L^+ case, we conclude from the figures that the photoproduction rate is much larger than the electroproduction rate (note again that we did not include the additional suppres-

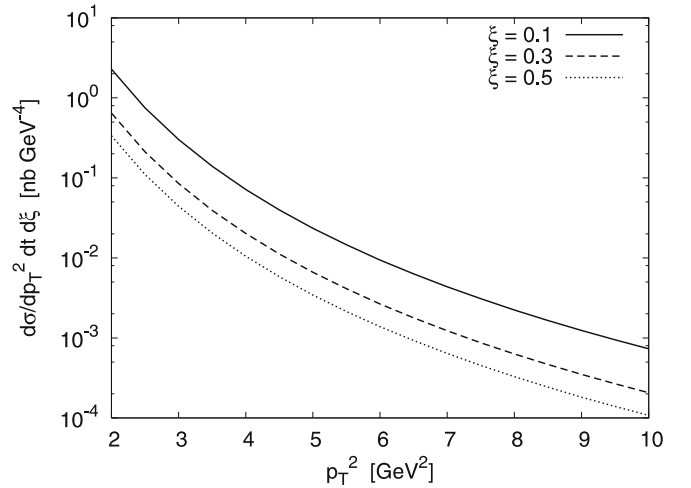


Fig. 6. The differential cross section for photoproduction of ρ_L^0, ρ_T^+ as a function of p_T^2 for $\xi = 0.1, 0.3,$ and 0.5

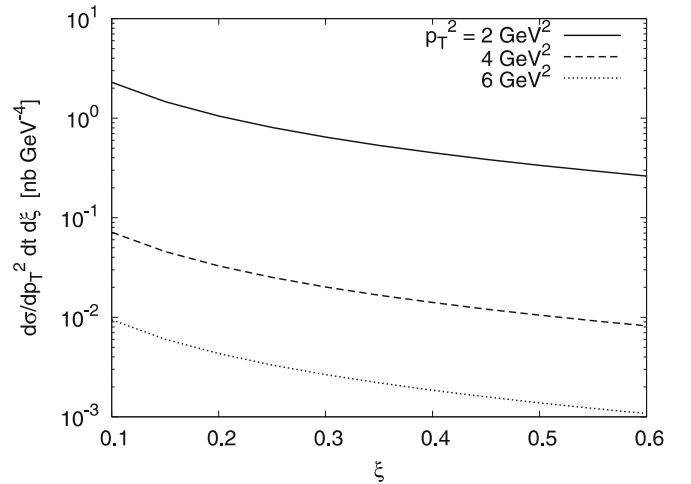


Fig. 7. The differential cross section for the photoproduction of transversely polarized ρ^0 and ρ^+ as a function of ξ for $p_T^2 = 2, 4,$ and 6 GeV^2

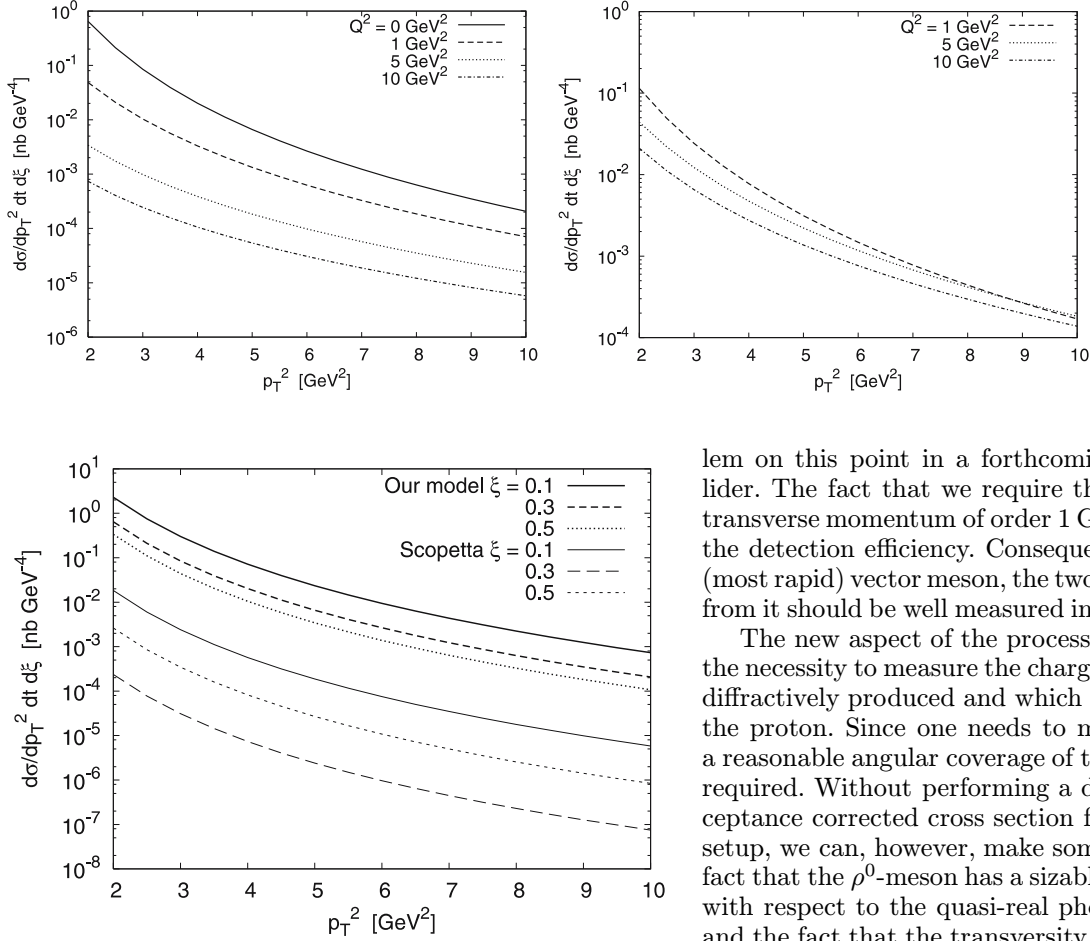


Fig. 8. The differential cross section for $\gamma_{L/T}^*(Q)p \rightarrow \rho_L^0 \rho_T^+ n$ for the transverse virtual photon (*left*) and the longitudinal virtual photon (*right*), plotted as a function of p_T^2 for $\xi = 0.3$ and $Q^2 = 0, 1, 5, \text{ and } 10 \text{ GeV}^2$

Fig. 9. Comparison of photoproduction of ρ_L^0, ρ_T^+ computed using our model for H_T and the model of [13]

sion factor coming from the virtual photon flux). Figure 9 shows a comparison of the corresponding photoproduction cross sections computed using our model (29) for H_T and the bag model estimate of [13]. Figure 9 illustrates the strong sensitivity of the production rate with respect to the transversity GPD used, and also the different ξ -dependence of the two.

7 Discussion and conclusions

Up to now we have shown that the process discussed here has a sizable cross section with respect to the quite large luminosities of current and projected high energy electron accelerators. In addition, one should ask about the detection efficiency of existing or planned experiments in the kinematical region where the two vector mesons are produced. A crucial point in favor of a good detection efficiency of our process is the fact that the two vector mesons are produced with large transverse momentum. Let us detail this statement. Detecting a quasi-forward diffractively produced ρ^0 is now routine work for experimentalists at HERA and COMPASS, and we do not expect any prob-

lem on this point in a forthcoming electron-proton collider. The fact that we require that this ρ^0 have a finite transverse momentum of order 1 GeV or more will improve the detection efficiency. Consequently, regarding the first (most rapid) vector meson, the two charged pions emerging from it should be well measured in modern detectors.

The new aspect of the process that we have studied is the necessity to measure the charged ρ -meson, which is not diffractively produced and which travels in the vicinity of the proton. Since one needs to measure its polarization, a reasonable angular coverage of the two outgoing pions is required. Without performing a detailed study of the acceptance corrected cross section for a given experimental setup, we can, however, make some definite remarks. The fact that the ρ^0 -meson has a sizable transverse momentum with respect to the quasi-real photon (i.e. lepton) beam, and the fact that the transversity GPD is peaked at small values of t , favors the case of a ρ^+ -meson with a similarly sizable transverse momentum (say greater than 1 GeV), which is shared between both emerging pions. This is good news with respect to the detection of these pions. To go further, one should distinguish between fixed target experiments, such as COMPASS and collider experiments such as H1 or ZEUS. In the first case, the longitudinal momentum of the ρ^+ -meson is (in the laboratory frame) of the order of $\sqrt{s_{\gamma p}}$, which is a few GeV, so that the emission angles of the ρ^+ -meson and hence those of the two π -mesons are within the acceptance of the spectrometer. In the collider kinematics, the efficiency may not be as good, since the vector meson is boosted along the direction of the proton beam. Note, however, that its longitudinal momentum is proportional to ξ , so that there is a small ξ region where the emerging mesons should not be hidden in the dead cone around the proton beam. These positive remarks do not mean that a detailed analysis is not needed, neither that special care is not required to improve the detection efficiency as much as possible, but they allow us to be quite optimistic about the feasibility of the proposed experiment.

We believe that the possible eRHIC machine may become the best place where the process discussed here can be measured, provided that experimental setups allow a large angular coverage, ensuring a sufficient detection efficiency and a good control of exclusivity. The JLab CLAS-12 upgrade will probably have good enough detection efficiency for observing the two rho-mesons, but only for relatively low

p_T of the order of 1–1.5 GeV. Moreover, the smaller energy available prevents the theoretical framework used here from being adequate and one needs to supplement our studies by adding contributions coming from other polarization states of exchanged gluons and the ones coming from quark exchanges. This we leave for future work.

The experimental measurement of the transversity GPD can thus supplement the intense present activity to unravel the transverse spin structure of the nucleon. An experimental determination of the transversity GPD H_T seems feasible in photoproduction or electroproduction at high energies, if the accelerator luminosity is of the order of what is anticipated at a future high-energy electron-proton collider.

Acknowledgements. We thank S. Scopetta for providing us with the parameterization of the GPD from [13]. We acknowledge useful discussions on experimental prospects with H. Avagyan, E. Burtin, J. Ciborowski, F. Kunne, A. Sandacz, L. Schoeffel and J. Ukleja. We also thank P. Hägler, D. Ivanov and O.V. Teryaev for helpful discussions. This work was supported in part by the Polish Grant 1 P03B 028 28, the French–Polish scientific agreement Polonium, the Joint Research Activity “Generalised Parton Distributions” of the European I3 program Hadronic Physics, contract RII3-CT-2004-506078, and the Swedish Research Council. L.Sz. is a Visiting Fellow of the Fonds National pour la Recherche Scientifique (Belgium).

References

1. J.P. Ralston, D.E. Soper, Nucl. Phys. B **152**, 109 (1979); X. Artru, M. Mekhfi, Z. Phys. C **45**, 669 (1990); J.L. Cortes, B. Pire, J.P. Ralston, Z. Phys. C **55**, 409 (1992); R.L. Jaffe, X.D. Ji, Phys. Rev. Lett. **67**, 552 (1991)
2. V. Barone, A. Drago, P.G. Ratcliffe, Phys. Rept. **359**, 1 (2002); M. Anselmino, arXiv:hep-ph/0512140
3. A.V. Belitsky, D. Müller, Phys. Lett. B **417**, 129 (1998); P. Hoodbhoy, X.D. Ji, Phys. Rev. D **58**, 054006 (1998); M. Diehl, Eur. Phys. J. C **19**, 485 (2001); M. Diehl, T. Gousset, B. Pire, Phys. Rev. D **59**, 034023 (1999); J.C. Collins, M. Diehl, Phys. Rev. D **61**, 114015 (2000); M. Diehl, P. Hägler, Eur. Phys. J. C **44**, 87 (2005)
4. D.Y. Ivanov, B. Pire, L. Szymanowski, O.V. Teryaev, Phys. Lett. B **550**, 65 (2002)
5. L.N. Lipatov, Sov. J. Nucl. Phys. **23**, 338 (1976); E.A. Kuraev, L.N. Lipatov, V.S. Fadin, Sov. Phys. JETP **44**, 443 (1976); E.A. Kuraev, L.N. Lipatov, V.S. Fadin, Sov. Phys. JETP **45**, 199 (1977); I.I. Balitsky, L.N. Lipatov, Sov. J. Nucl. Phys. **28**, 822 (1978)
6. P. Ball, V.M. Braun, Phys. Rev. D **54**, 2182 (1996)
7. M. Diehl, Eur. Phys. J. C **19**, 485 (2001)
8. A.V. Radyushkin, Phys. Rev. D **59**, 014030 (1999)
9. M.V. Polyakov, C. Weiss, Phys. Rev. D **60**, 114017 (1999)
10. K. Goeke, M.V. Polyakov, M. Vanderhaeghen, Prog. Part. Nucl. Phys. **47**, 401 (2001)
11. A.D. Martin, R.G. Roberts, W.J. Stirling, R.S. Thorne, Phys. Lett. B **604**, 61 (2004)
12. R.L. Jaffe, X.D. Ji, Phys. Rev. D **43**, 724 (1991)
13. S. Scopetta, Phys. Rev. D **72**, 117502 (2005) See also B. Pasquini, M. Pincetti, S. Boffi, Phys. Rev. D **72**, 094029 (2005)
14. QCDSF Collaboration, M. Göckeler et al., Phys. Lett. B **627**, 113 (2005)
15. L. Mankiewicz, G. Piller, A. Radyushkin, Eur. Phys. J. C **10**, 307 (1999)
16. L.P. Gamberg, G.R. Goldstein, Phys. Rev. Lett. **87**, 242001 (2001)